Carbohydrate Polymers 82 (2010) 256–263

Contents lists available at ScienceDirect

Carbohydrate Polymers

journal homepage: www.elsevier.com/locate/carbpol

Thermoplastic starch plasticized by an ionic liquid

Abdulkader Sankri[a], Abdellah Arhaliass[a], Isabelle Dez[b], Annie Claude Gaumont[b], Yves Grohens[c], Denis Lourdin[d], Isabelle Pillin[c], Agnès Rolland-Sabaté[d], Eric Leroy[a,*]

[a] Laboratoire GEPEA, UMR CNRS 6144, Université de Nantes, 37 bd de l'université, 44606 St Nazaire, BP 420 cedex, France
[b] Laboratoire de Chimie Moléculaire et Thio-organique, UMR CNRS 6507, INC3M, FR 3038, ENSICAEN & Université de Caen, 14050 Caen, France
[c] Laboratoire LIMATB, rue de Saint Maudé, BP 92116, 56321 Lorient cedex, France
[d] Unité BIA, Inra, BP 71627, 44316 Nantes cedex 03, France

ARTICLE INFO

Article history:
Received 16 March 2010
Received in revised form 2 April 2010
Accepted 13 April 2010
Available online 20 April 2010

Keywords:
Thermoplastic starch
Ionic liquids
Interactions
Mechanical properties
Plasticization
Electrical conductivity

ABSTRACT

Thermoplastic starch (TPS) plasticized by 1-butyl-3-methylimidazolium chloride ([BMIM]Cl) was obtained by melt processing. The resulting electrically conductive TPS samples were less hygroscopic than glycerol plasticized TPS samples. Despite this lower water uptake, [BMIM]Cl seems to be intrinsically a more efficient plasticizer of starch. [BMIM]Cl plasticized TPS samples show a much higher elongation at break in the rubbery state than the glycerol plasticized TPS samples. Their unusually low rubbery Young's modulus for thermoplastic starch (0.5 MPa) suggests a strong reduction of hydrogen bonds between the starch chains due to the presence of the ionic liquid. A detailed IR spectroscopy analysis supports this interpretation.

1. Introduction

A recent synthetic review was dedicated to thermoplastic starch (TPS) polymers (Halley et al., 2008, Chap. 24). Unlike polymers with added granular starch, TPS is obtained by destructuration of native starch granules. This irreversible order–disorder transition termed gelatinization can be either obtained by solubilizing starch in water or by treating starch granules thermo-mechanically in the presence of water. TPS is thus obtained by film casting or by extrusion.

Halley et al. (2008, Chap. 24) list the current commercial applications of TPS polymers. In most cases, traditional polymer markets are concerned, such as packaging, films and some engineering applications. Consequently, the properties of TPS that are generally considered are mechanical properties and sensitivity to water.

On the other hand, new high added value applications for TPS materials are being explored such as drug delivery (Piskin, 2002), tissue engineering (Piskin, 2002), electroactive polymers (Finkenstadt & Willett, 2004), shape memory polymers (Véchambre, Chaunier, & Lourdin, 2010) or solid polymer electrolytes (Ma, Yu, & He, 2006). For this last objective, a promising approach is described by Wang, Zhang, Liu, and He (2009). The ionic liquid (1-allyl-3-methylimidazolium) chloride ([AMIM]Cl) was used as a plasticizer of starch in films obtained by casting from aqueous solutions. Levels of electrical conductivity up to $10^{-1.6}$ S/cm were obtained for 30 wt% of [AMIM]Cl at 14.5 wt% water content. The preparation of ion conductive starch films using ionic liquids had been previously reported by Nishimura and Ono (2005) in a short preprint article.

Ionic liquids (ILs) are low melting point salts, which have attracted much interest in the last years in academy and in industry (Robin, Rogers, Seddon, & Volkov, 2003), due to their enormous potential as "green" recyclable substitutes for the traditional organic solvents (Rogers & Seddon, 2003; Sheldon, 2001; Welton, 1999). Being entirely composed of ions, they possess negligible vapour pressure and are non-flammable. Moreover, ILs can be tailored by modifying the chemical structure of the cation and anion moieties, in order to dissolve solutes of a wide-range of polarities and show varied miscibility with other solvents (Anderson, Ding, Welton, & Armstrong, 2002; Brennecke, Rogers, & Seddon, 2007).

Since less than a decade, ILs have found a wide application in the dissolution of carbohydrates such as cellulose (Swatloski, Spear, Holbrey, & Rogers, 2002; Zhu et al., 2006), lignocellulosic materials (Fort et al., 2007; Kilpeläinen et al., 2007), starch (Biswas, Shogren, Stevenson, Willett, & Bhowmik, 2006) and chitin and chitosan (Xie, Zhang, & Li, 2006). Some hydrophilic ILs can dissolve cellulose and other polysaccharides in high concentrations (Fort et al., 2007; Swatloski et al., 2002; Swatloski, Rogers, & Holbrey, 2003; Zhang, Wu, Zhang, & He, 2005). The detailed knowledge of

* Corresponding author. Tel.: +33 0240172660; fax: +33 0240172618.
E-mail address: eric.leroy@univ-nantes.fr (E. Leroy).

0144-8617/$ – see front matter © 2010 Elsevier Ltd. All rights reserved.
doi:10.1016/j.carbpol.2010.04.032

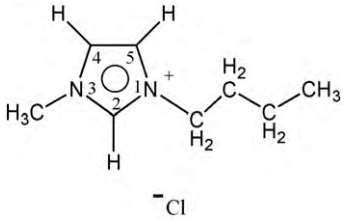

Fig. 1. Structure of 1-butyl-3-methylimidazolium chloride ([BMIM]Cl).

the solvation of carbohydrates in ILs is not known. However, it has been shown by NMR spectroscopy and molecular dynamics that solvation involves the formation of hydrogen bonds between the anions of the imidazolium salts and the hydroxyl group protons of the sugar in approximately a stoichiometric ratio (Moulthrop, Swatlowski, Moyna, & Rogers, 2005; Novoselov, Sashina, Petrenko, & Zaborsky, 2007; Remsing, Swatlowski, Rogers, & Moyna, 2006; Youngs et al., 2006; Youngs, Hardacre, & Holbrey, 2007). Thus, imidazolium ILs bearing hydrophilic anions are media capable to dissolve carbohydrates (Fukaya, Sugimoto, & Ohno, 2006; Fukaya, Hayashi, Wada, & Ohno, 2008; Heinze et al., 2008; Liu, Janssen, van Rantwijk, & Sheldon, 2005). The specific function of the cation is however less understood. All that can be said is that the role of the cation in the dissolution mechanism appears to be secondary and related mainly to its size and hydrophobicity (Remsing et al., 2006; Swatloski et al., 2002). The possible dissociation of the ion pairs also plays an important role in some cases (Zhang et al., 2005).

Most of the published works focus on the dissolution of cellulose. It has been shown for example, that (1-allyl-3-methylimidazolium) chloride ([AMIM]Cl) is a better solvent of cellulose than (1-butyl-3-methylimidazolium) chloride ([BMIM]Cl) (Zhang et al., 2005). The better solubilization of cellulose by [AMIM]Cl is attributed not only to the smaller size and higher polarity of the $[AMIM]^+$ cation, but also to an ion pair dissociation mechanism above a critical temperature (42 °C in pure[AMIM]Cl) (Zhang et al., 2005). $[AMIM]^+$ and Cl^- ions are therefore more able to interact individually with oxygen and hydrogen atoms of different O–H groups of cellulose, respectively.

On the contrary, in [BMIM]Cl, the ion pairs are more stable. [BMIM]Cl in the anhydrous state has a high temperature of fusion (T_f = 67 °C). Nevertheless, in contact with ambient air, it becomes liquid at room temperature due to water uptake. In the ionic liquid [BMIM]Cl, the Cl^- anions preferentially interact with the hydrogen atoms attached to C(2), C(4) and C(5) of the $[BMIM]^+$ imidazolium ring (Fig. 1). The probability of location of the anion close to C(2) or close to C(4) and C(5) depends on the environment.

Hanke, Atamas, and Lynden-Bell (2002) used molecular dynamics to study the dissolution of polar molecules (water and methanol) and non-polar molecules (dimethyl ether and propane) in [BMIM]Cl. They showed that for polar molecules, the strongest interactions are hydrogen bonds between the Cl^- anions and the hydrogen of –O–H groups. The complex formed interacts with the $[BMIM]^+$ cations. In the most probable spatial configuration, the oxygen atom is preferentially attracted by the hydrogen attached to C(4) and C(5) of the imidazolium ring. The hydrogen attached to the C(2) remains closer to the Cl^- anion.

Hanke et al. (2002) showed that in the case of non-polar molecules, the strongest interaction involves the $[BMIM]^+$ cation. In the case of dimethyl ether, the oxygen atom of the ether function is attracted by the hydrogen attached to C(4) and C(5) of the imidazolium ring.

Novoselov et al. (2007) simulated the dissolution of cellulose in BMIM[Cl]. They showed the formation of hydrogen bonds between one Cl^- anion and three hydrogen atoms located: on a C–O–**H** group of cellulose, on a CH_2–O–**H** group of cellulose (on the same chain or another chain), and on the C-2 carbon of the imidazolium ring. These interactions explain why the inter- and intra-molecular hydrogen bonds between C–O–H and CH_2–O–H groups of cellulose are broken by [BMIM]Cl, which solubilized the polysaccharide.

The interactions of ionic liquids with starch were much less studied. Biswas et al. (2006) showed that BMIM[Cl] can be used as a solvent at 80 °C up to 15 wt%. In the aforementioned work of Wang et al. (2009), [AMIM]Cl was used as a plasticizer of starch in films obtained by casting from aqueous solutions. In particular, they observed that ([AMIM]Cl) plasticized starch films are more hygroscopic than classical glycerol plasticized films and that very high levels of electrical conductivity are obtained in the presence of [AMIM]Cl (up to $10^{-1.6}$ S/cm at 14.5 wt% water content). Wang et al. (2009) also discuss the interactions between starch and the ionic liquid in terms of hydrogen bonding, studied by infrared spectroscopy. In an another recent article (Wang, Zhang, Liu, & Han, 2010), they show that the addition of LiCl in cast films increases the interactions between [AMIM]Cl and starch, as well as the electrical conductivity and the water uptake.

In the present work, we studied the plasticization of starch by [BMIM]Cl. Our first objective was to show the feasibility of plasticizing starch by an ionic liquid, by melt processing. Two processing scales were used: A twin screw extruder was used to evaluate the feasibility of melt processing ionic liquid plasticized starch on an industrial scale. Nevertheless, from a research perspective, it was also important to be able to investigate the plasticization of starch on very small quantities using a microcompounder. Such a small processing scale opens the door for a high-throughput approach of the synthesis of tailored ionic liquids for plasticization.

Our second objective was to contribute to the study of the interactions between starch and ionic liquids and their influence on functional properties (water uptake, mechanical and electrical properties) of the thermoplastic starch obtained.

2. Experimental

2.1. Materials and processing

Maize starch was purchased from Tate & Lyle (Meritena 100). The initial moisture content was 12 wt%. Plasticizers used were glycerol (technical grade, CHIMIPHAR) and [BMIM]Cl, purchased in crystallized form under argon atmosphere (Solvionic, France).

Thermoplastic starch (TPS) samples were prepared by thermomechanical transformation of starch in the presence of plasticizers (glycerol and/or [BMIM]Cl) and water. Two series of samples have been prepared by melt processing (Table 1). Two processing scales have been used: A laboratory scale microcompounder allowing the preparation of batches of typically 5–10 g of TPS, and a twin screw extruder allowing continuous production.

In Table 1, MC or EXT indicates that the sample was obtained using the microcompounder (MC) or the twin screw extruder (EXT), respectively. The letters S (for starch), G (for glycerol) and B (for [BMIM]Cl) are followed by their proportions in dry weight in the sample. For example: [MC S100-G15-B15] means a sample prepared using the microcompounder, containing 100 g of starch, 15 g of glycerol and 15 g of ionic liquid.

Table 1
Proportions of glycerol and BMIMCl used for the preparation of TPS samples (%).

Sample	Starch	Glycerol	[BMIM]Cl
[MC S100-G30]	100	30	0
[MC S100-B30]	100	0	30
[MC S100-G15-B15]	100	15	15
[EXT S100-G30]	100	30	0
[EXT S100-B30]	100	0	30

2.1.1. Microcompounder

The Minilab microcompounder (Thermo Haake) is a conical twin screw system with a backflow channel. This allows using the Minilab as a batch mixing reactor given that the material can be recirculated rather than exiting through the die. In the mean time, the conical twin screw system allows to simulate the performance of a co-rotating or a counter rotating twin screw extruder. In all operations, the co-rotation operation was applied.

The following procedure was used: starch (S) powder (12% water) was premixed with glycerol (G) and/or [BMIM]Cl (B) in a mortar and then introduced in the microcompounder at 160 °C (this high temperature was chosen due to the low moisture level), at low rotation speed (40 rpm) of the twin co-rotating screws in less than 2 min. Then the (recirculating) mixing was continued for 2 min at 100 rpm and then the TPS was extruded through the exit die.

2.1.2. Twin screw extrusion

A Clextral BC21 corotating twin screw extruder was used. The starch powder (12% water) was introduced at the feed port of the extruder using a volumetric feeder. In the same feeding zone, the liquid plasticizers (glycerol or water solution of [BMIM]Cl (17%, w/w%)) were pumped to the extruder through a peristaltic pump. The average feeding rate was 1 kg/h. In the feeding zone, the temperature was 90 °C, increasing up to 120 °C at the die exit. The screw speed employed was 300 rpm. The extruded thermoplastic material was collected and placed in sealed bags.

2.1.3. Film processing and storage

In both cases, after melt processing, the samples were thermomoulded into films at 110 °C for 5 min and cooled down to 60 °C under pressure. The films obtained had a typical thickness of 500 μm. They were stored at 25 °C under a controlled relative humidity of 50%. The increasing weight of each film (due to water uptake) was measured regularly. No more variations were observed after 3 days, showing that the equilibrium water uptake (at 50% R.H.) was reached, allowing the characterization of the samples.

2.2. Characterization

All characterizations were conducted on samples obtained by twin screw extrusion and thermomoulding, cut from the films at equilibrium (50% R.H.). The samples obtained using the microcompounder were only analysed by infrared spectroscopy due to insufficient quantities for the preparation of tensile test samples.

2.2.1. Macromolecular characterizations of the extruded samples

High Performance Size Exclusion Chromatography coupled with Multi-Angle Laser Light Scattering and Quasi-Elastic Light Scattering (HPSEC–MALLS–QELS) were used. The samples were solubilized using the method previously described by Bello-Pérez, Roger, Baud, and Colonna (1998). The films were DMSO-pre-treated, dried and solubilized by microwave heating under pressure. Each sample suspension in water at a concentration of 0.5 g L^{-1} was heated for 40 s (maximal internal temperature reached: 152 °C) at 900 W. Starch solutions were then filtered through 5 μm Durapore™ membranes (Waters, Bedford, MA, USA). Carbohydrate concentrations were determined by the sulphuric acid-orcinol colorimetric method described by Planchot, Colonna, and Saulnier (1997). Sample recoveries were calculated from the ratio of the initial mass and the mass after filtration. Solutions were immediately injected into the HPSEC–MALLS–QELS system. The equipment and the method used were the same as that described previously (Rolland-Sabaté, Colonna, Mendez-Montealvo, & Planchot, 2008), except the SEC column used. The SEC column was Shodex® KW-802.5 (8 mm ID × 30 cm) together with a KW-G guard column (6 mm ID × 5 cm) both from Showa Denko K.K. (Tokyo, Japan). They were maintained at 30 °C. The two on-line detectors were a Dawn® Heleos® MALLS system fitted with a K5 flow cell and a GaAs laser, (λ = 658 nm), supplied by Wyatt Technology Corporation (Santa Barbara, CA, USA) and an ERC-7515A refractometer from Erma (Tokyo, Japan). On-line QELS measurements were performed using a WyattQELS® system supplied by Wyatt Technology Corporation and included in the Dawn® Heleos®. QELS measurements were performed at 142.5° for a time interval of 7 s. Before use, the mobile phase (Millipore water containing 0.2 g L^{-1} of sodium azide) was carefully degassed and filtered through Durapore GV (0.2 μm) membranes from Millipore (Millipore, Bedford, MA, USA), and eluted at a flow rate of 0.3 mL min^{-1}. Sample recovery rates were calculated from the ratio of the mass eluted from the column (integration of the DRI signal) and the mass injected. Injected masses were determined using the sulfuric acid-orcinol colorimetric method (Planchot et al., 1997). $\bar{M}_n$, $\bar{M}_W$, the polydispersity index, $\bar{M}_W/\bar{M}_n$, $\bar{R}_G$ (nm) and $\bar{R}_H$ (nm) were established using ASTRA® software from WTC (version 5.3.4.14 for PC) (Wyatt, 1992), as previously described by Rolland-Sabaté, Amani, Dufour, Guilois, & Colonna, 2003; Rolland-Sabaté et al., 2008. A value of 0.145 ml g^{-1} was used as the refractive index increment (d*n*/d*c*) for glucans and the normalization of photodiodes was achieved using a low molar mass pullulan standard (P20). Only [EXT S100-G30] and [EXT S100-B30] TPS samples were analysed using this technique, to evaluate the effect of twin screw extrusion.

2.2.2. Characterization of thermoplastic starch films

The *water content* of the films was measured by weight loss after drying on samples of 1 g in an oven at 130 °C for 4 h. No significant additional weight losses were observed for longer drying times.

The *glass transition temperature* was measured by differential scanning calorimetry on samples of typically 10 mg. The glass transition temperature was defined as the onset of the heat capacity increase. In the first series of experiments, samples (conditioned at equilibrium at 50% R.H.) were placed on sealed capsules and cooled to −50 °C before applying a temperature ramp up to 100 °C at 10 °C/min. No water crystallization or fusion peaks were detected. In the second series of experiments, the samples were placed on opened capsules and heated from 20 °C up to 150 °C in order to dry the samples, which were then cooled to 20 °C and heated again up to 150 °C at 10 °C/min. The glass transition temperatures, referred as "*dry*" T_g were observed between 50 and 100 °C.

The *DC bulk electrical conductivity* was measured using an electrometer (KEITHLY Hioki-3522-LCR Hitester), applying a voltage between 0 and 5 V on film samples ($10 \times 16 \times 0.5$ mm^3).

The *infrared absorption spectra* of the films were obtained with a resolution of 1 cm^{-1} in the 700–4000 cm^{-1} wave number range, using a Fourier Transform Infrared (FTIR) Spectrometer (Tensor 27, BRUKER) equipped with an Attenuated Total Reflection system (ATR, PIKE). The OPUS® software was used for the analysis of the IR absorption spectra, especially for the identification of peak maxima.

Mechanical tensile tests were conducted on ASTM D412 type dogbone sampled cut from the films, using an INSTRON 1122 universal press at 10 mm/min. No extensometer could be used due to the sticky behaviour of the samples. The strain was defined as the ratio of the displacement of cross-head *x* to the initial length of the sample l_0.

$$\varepsilon = \frac{x}{l_0}$$

The stress was defined as the ratio of the force *F* to the initial section of the sample S_0

$$\sigma = \frac{F}{S_0}$$

The stress–strain curve was analysed in order to obtain the *Elongation at break* (%), the *Rupture stress* (MPa) and the *Elastic*

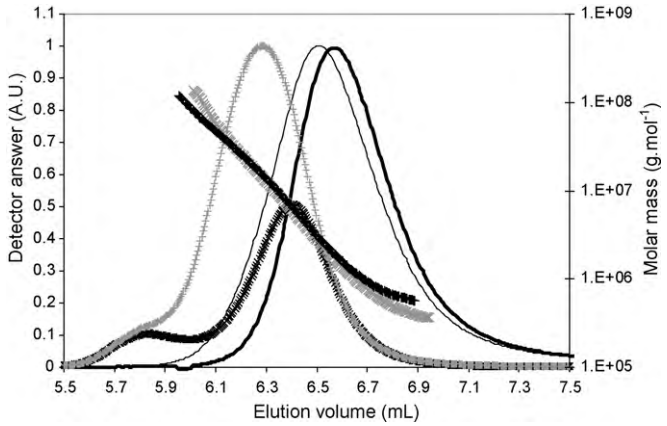

Fig. 2. Chromatograms of TPS samples (LS and DRI answer) and molar masses versus elution volume. [EXT S100-B30] LS, DRI answer and molar masses (×, thick line and × (grey crosses) respectively), [EXT S100-G30] LS, DRI answer and molar masses (+ (grey plus), thin line and + respectively).

modulus (MPa) defined as the secant modulus at 5% elongation.

3. Results and discussion

3.1. Influence of [BMIM]Cl on macromolecular structure

Concerning the *macromolecular characterization*, the DMSO pretreatment recoveries were 100% for [EXT S100-G30] and [EXT S100-B30]. This DMSO pretreatment is known to remove the polysaccharide oligomers whose degree of polymerisation (DP) is smaller than 12. Then, this recovery of 100% shows that in both cases the extrusion treatment does not induce the apparition of sugars with DP smaller than 12, because of the starch degradation during extrusion. The solubilization recovery rates and the elution recoveries of extruded starches were 100%. The high sample recovery values obtained here indicate that the fractionation response was quantitative for all the samples. This solubilization mode was thus considered as enabling the representative structural characterisation of these starches.

TPS sample's chromatograms showed two light scattering (LS) peaks at elution volumes (Ve) of 5.8 mL and 6.3–6.4 mL (Fig. 2), and displayed a single differential refractive index (DRI) peak at a Ve of 6.5–6.7 mL, corresponding to the major part of the sample. For both samples, the LS peaks are shifted to smaller elution volumes compared to the DRI peak. This means that the sample is polydisperse and that there are very small quantities of big molecules (the smaller the elution volume, the bigger the size of the molecule). Consequently, the first LS peak at Ve 5.8 mL is attributed to residual non-degraded or slightly degraded amylopectin fraction. Then, the main DRI peak, corresponding to the major part of the TPS sample, corresponds to highly degraded amylopectin molecules. No additional peak corresponding to DP lower than 600 was observed.

Both TPS samples present average molar masses and radii lower than native normal maize starch (Table 2) which have been reported to have a molar mass of 1.85×10^8 g mol^{-1} for normal maize and a radius of gyration of 238 nm (Rolland-Sabaté et al., 2003). This confirms that molecular degradation occurred in both cases during the process. This is in agreement with literature data about extrusion of starches with water or glycerol (Myllymäki et al., 1997; Van den Einde, van der Veen, Bosman, van der Goot, & Boom, 2004a, 2004b).

For [EXT S100-B30], LS and DRI peaks are shifted to higher elution volumes compared to [EXT S100-G30] (Fig. 2), meaning that [EXT S100-B30] displays smaller sizes. This is confirmed by the data reported in Table 2 where the molar mass and the radius reported are smaller for [EXT S100-B30] than for [EXT S100-G30].

By plotting the hydrodynamic radii and the molar masses of the same fraction, structural data could be determined from the exponent ν_H in the equation: $R_{Hi} = K_H \times M_i^{\nu_H}$. The ν_H value depends on polymer shape, temperature and polymer–solvent interactions: $\nu_H = 0.33$ for a sphere, $\nu_H = 0.5$–0.6 for a linear random coil and $\nu_H = 1$ for a rod, according to Flory theory (Flory, 1953). A very good fit of experimental data is achieved using previous equation. The ν_H values calculated for TPS samples are 0.34 for [EXT S100-G30] and [EXT S100-B30] (Table 2). These values are close to the value for a compact sphere indicating a very dense branching structure and are in good agreement with data reported in the literature for amylopectin (Roger, Bello-Pérez, & Colonna, 1999). ν_H values are the same for [EXT S100-G30] and [EXT S100-B30] meaning that the structures of these macromolecules are similar.

In summary, the extrusion process with [BMIM]Cl induces a higher decrease in molar mass and in size than extrusion with glycerol does. However, the branching structure of the degraded starches is similar to both extrusion processes. And, no short DP was produced during these two extrusion processes.

The derivatizing or non-derivatizing behaviour ionic liquids toward polysaccharides have been studied in the last decade. [BMIM]Cl was shown to degrade cellulose by Laus et al. (2005). After regeneration from solution of 25% by weight of cellulose in BMIM[Cl] at 100 °C, a decrease of the molecular weight by 1–2 orders of magnitude of the polysaccharide molecular weight was observed. As an opposition, when [AMIM]Cl was used, no degradation of cellulose could be observed.

If we now focus on starch, Biswas et al. (2006) showed that BMIM[Cl] can be used as a solvent at 80 °C up to 15% weight. Nevertheless, the depolymerization of amylopectin by [BMIM]Cl was later observed for starch of different botanical sources by Stevenson, Biswas, Jane, and Inglett (2007). [BMIM]Cl was shown to reduce the amylopectin molecular weight of starches when dissolved in the ionic liquid and stored at 100 °C during 1 h before being recovered by precipitation with ethanol. For cereal starches (including corn), 4–6 peaks were observed in molecular weight chromatograms obtained by high-performance size-exclusion chromatography (HPSEC) for regenerated starch samples. The corresponding molecular weights were down to 4 orders of magnitude lower than the initial reference peak observed

Table 2
Weight average molar mass ($\bar{M}_W$), *z* average hydrodynamic radius ($\bar{R}_H$), hydrodynamic coefficient (ν_H) and polydispersity index ($\bar{M}_W/\bar{M}_n$) determined by HPSEC–MALLS–QELS for TPS samples.

	Modal population		Whole population				Integration range	
Samples	$\bar{M}_W \times 10^{-6}$ (g mol^{-1})	$\bar{R}_H$ (nm)	$\bar{M}_W \times 10^{-6}$ (g mol^{-1})	$\bar{R}_H$ (nm)	ν_H	$\bar{M}_W/\bar{M}_n$	$M_i \times 10^{-6}$ (g mol^{-1})	V_i (mL)
[EXT S100-G30]	2.94	26.7	6.82	49.6	0.34	3.71	123–0.56	5.95–6.90
[EXT S100-B30]	2.09	23.7	3.15	39.4	0.34	3.02	139–0.37	6.00–6.95

The modal population corresponds to the major part of the sample: the data were taken at the apex of the refractometric peak. The integration range corresponds to the whole population. The experimental uncertainties on $\bar{M}_W$, $\bar{M}_W/\bar{M}_n$ and $\bar{R}_H$ values are 5%.

Table 3
Water uptake, glass transition temperatures, DC electrical conductivities and mechanical properties of the extruded samples stored at 50% R.H. at equilibrium.

Sample	[EXT S100-G30]	[EXT S100-B30]
Water content measured (wt%)	20 (±1)	13 (±1)
Plasticizer content calculated (wt%)	25	25
Starch content calculated (wt%)	55	62
T_g measured (°C)	−21	−13
T_g calculated (°C)	−36	−6
"Dry" T_g measured (°C)	80	48
"Dry" T_g calculated (°C)	91	91
Electrical conductivity (S/cm)	$10^{-5.4}$	$10^{-4.6}$
Young's modulus (MPa)	8.3 (±0.9)	0.5 (±0.1)
Stress at break (MPa)	1.9 (±0.1)	0.6 (±0.1)
Strain at break (%)	88 (±7)	392 (±27)

for the native starches (Stevenson et al., 2007). From those results, the authors conclude that [BMIM] Cl may have limited applications as a solvent for starch.

Actually a patent published in 2005 (Myllymäki & Aksela, 2005) claims that the depolymerization of starch can be selective. Depending on the temperature and stirring time, the patent shows examples of selective depolymerization of amylose, amylopectin remaining intact (for stirring for 30 min at 85 °C and 2 h at 100 °C), or complete depolymerization of both polysaccharides (for stirring for 30 min at 85 °C and 2 h at 100 °C). All the examples are given for barley starch samples and the ionic liquid [BMIM]Cl. The authors insist that very low amounts of water should be present, typically lower than 1 percent by weight.

Our results clearly show that when thermoplastic starch is melt processed with [BMIM]Cl, no such depolymerization occurs as no short DP was observed. The smaller macromolecular weight values observed (compared to glycerol plasticized thermoplastic starch) may be related to a small derivatizing effect of [BMIM]Cl. Nevertheless, the decrease in macromolecular weight observed seems to be mainly the result of the thermo-mechanical treatment.

3.2. Influence of [BMIM]Cl starch plasticization

Water uptake and glass transition temperatures measured on the extruded samples equilibrated at 25 °C, 50% RH are shown in Table 3. The thermoplastic starch containing [BMIM]Cl is less hydrophilic than the classical glycerol plasticized TPS. They contain 13% and 20% water respectively. This result can seem surprising given the strong hydrophilic nature of the ionic liquid. Nevertheless, we also measured the water uptake of pure [BMIM]Cl and pure glycerol at 50% R.H. For both compounds, the moisture content was around 36 wt%. Consequently, the decrease of the TPS water uptake in the presence of [BMIM]Cl may be related to a specific interaction mechanism with starch, limiting the interactions of the polysaccharide with water molecules.

The glass transition of samples containing glycerol or [BMIM]Cl was measured after water equilibration and after drying. In parallel the glass transition temperature of the mixtures has been calculated using the Couchman–Karasz relation (Couchman & Karasz, 1978):

$$T_{g_{mix}} = \frac{\sum X_i \Delta C_{p_i} T_{g_i}}{\sum X_i \Delta C_{p_i}}$$

where X_i is the weight fraction of constituent i, T_{g_i} is the glass transition temperature of the pure constituent i, and ΔC_{p_i} is the variation of the heat capacity at T_{g_i} of the pure constituent i. The values ΔC_{p_i} and T_{g_i} come from a previous study (Lourdin, Coignard, Bizot, & Colonna, 1997).

The T_g of different mixtures studied has been calculated from the ternary composition starch/glycerol/water as indicated in Table 3. Plasticizer and starch composition have been deduced from the starch/glycerol ratio introduced, and the water content measured. For starch plasticized by glycerol, the T_g calculated at −36 °C is lower than the experimental T_g determined at −21 °C. This deviation could be imputed to the demixing of plasticizer evidenced for high plasticizer contents in a previous work (Lourdin et al., 1997).

Concerning the dry sample its T_g calculated at 91 °C is higher than the experimental T_g determined at 80 °C. This deviation is attributed to a small quantity of water remaining in the sample. Water is known to be an extremely efficient plasticizer of starch. According to literature results, 1% of water content results in a decrease of about 10 °C of the glass transition temperature (Bizot et al., 1997).

Concerning starch plasticized by [BMIM]Cl, the T_g measured at −13 °C is lower than the T_g calculated at −6 °C in the case of plasticization by glycerol for a composition starch/glycerol/water of 62/25/13. This important result means that [BMIM]Cl has a better efficiency as T_g depressor of starch than the classic plasticizer glycerol. The same behaviour is observed on the dry sample. The T_g measured at 48 °C is much lower than the T_g calculated at 91 °C for a dry glycerol plasticized starch.

The glass transition of a polymer is theoretically dependent on its molar mass: the shorter the chains, the lower the T_g. Such a T_g dependence with molar mass has been previously studied on hydrolysed pea starch (Lafargue, Pontoire, Buléon, Doublier, & Lourdin, 2007). It showed that a decrease of the weight average molar mass from 1.60 to 0.59×10^6 g mol^{-1} (divided by 2.7) induces a weak decrease of about 4 °C on T_g. We can conclude that the differences of molar mass measured on glycerol and LI plasticized starch do not explain the large differences evidenced on the T_g and water sorption behaviour. Therefore, we conclude that [BMIM]Cl is intrinsically a much better plasticizer of starch than glycerol.

3.3. Interactions between [BMIM]Cl and starch

Fig. 3 shows the *Infrared absorption spectra* for TPS samples produced using the microcompounder and Table 4 gives the position of the maxima of the most significant peaks (for TPS samples both obtained with the microcompounder and the twin screw extruder).

The main characteristics of the Mid-infrared spectra of starch have been recently reviewed by Capron, Robert, Colonna, Brogly, and Planchot (2007). We will consider three ranges of wavenumbers:

- The 3000–3600 cm^{-1} region in which a broad absorption peak is associated with the stretching vibration mode of the hydrogen bonded O–H groups of starch and absorbed water.
- The 950–1200 cm^{-1} region, where are located the absorption peaks of the C–C and C–O stretching vibration modes and of the C–O–H bending modes.
- The 950–700 cm^{-1} region, where are located the C–O–C α(1–6) (and α(1–4)) stretching modes and the C–O–C ring breathing modes.

In the 1300–700 cm^{-1} region, all authors agree that it is not possible to assign the bands individually, due to highly coupled vibration modes (Capron et al., 2007).

Nevertheless, in order to compare the strength of the hydrogen bonds formed by different plasticizers with the oxygen atoms of starch, Yang, Yu, and Ma (2006), attribute characteristic peaks to stretching vibration modes of C–O bonds. The peaks at 1080 and 1150 cm^{-1} are attributed to the C–O bond stretching in the C–O–H groups of starch, while the peaks at 1000 and 1020 cm^{-1} are attributed to the C–O bond stretching in the C–O–C group of the anhydroglucose rings.

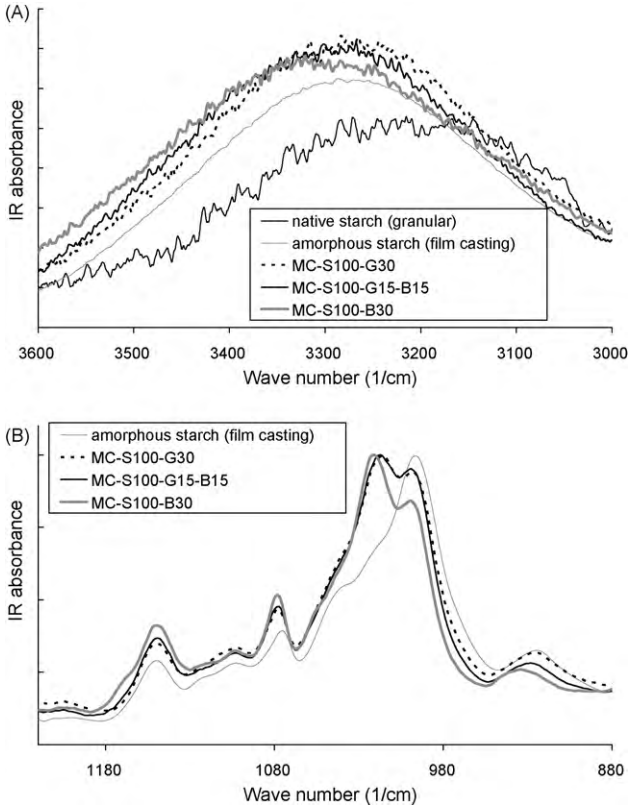

Fig. 3. FTIR spectra of plasticized starch obtained using the microcompounder process and comparison with reference samples (granular starch and starch film obtained by casting): (A) 3000–3600 cm^{-1} range and (B) 880–1200 cm^{-1} range.

By considering a simple harmonic oscillator model, the shift of these peaks toward lower wavenumbers indicates an increase of the hydrogen bonding to which the oxygen atoms of the C–O bonds in starch (Yang et al., 2006) are submitted. A similar shift toward lower wavenumbers of the maximum of the broad peak in the 3000–3600 cm^{-1} range will indicate an increase of the hydrogen bonding to which the hydrogen atoms of the O–H bonds in starch are submitted. As an opposition, a shift toward higher wavenumbers will indicate a decrease of hydrogen bonding (in the complete absence of hydrogen bonds, the stretching vibration mode of O–H groups should result in a narrow peak located in the 3645–3600 cm^{-1} range).

The broad IR absorption peak shown in Fig. 3A around 3300 cm^{-1} is associated with the stretching vibration mode of the hydrogen bonded O–H groups of starch (and of water and glycerol molecules). Table 4 gives the positions of the maximum of the peak calculated using the OPUS® software identification routine. The values obtained seem to indicate that the maximum of this peak is shifted toward higher wavenumbers in the presence of [BMIM]Cl. According to Yang et al. (2006), such a shift would be a signature of that, on average, the global strength of the hydrogen bonds to which the hydrogen atoms of the O–H groups are submitted become lower in the presence of [BMIM]Cl. Nevertheless, such results must be taken cautiously given the high level of noise in the spectra in this wavenumber range and because of the different water contents of the different samples. Perhaps a more significant signature of the interactions of [BMIM]Cl with OH groups is the width of the peak which increases from 391 cm^{-1} in the presence of glycerol ([MC S100-G30]) to 447 cm^{-1} in the presence of the ionic liquid ([MC S100-B30]).

Let us now consider the 800–1200 cm^{-1} range of wavenumber (Fig. 3B and Table 4). The maxima of the absorption peaks associated with the stretching vibration mode of the C–O bonds in C–O–C of anhydroglucose rings are shifted toward higher wavenumbers in the presence of [BMIM]Cl, indicating that the oxygen atoms of these groups are less hydrogen bonded than in glycerol plasticized starch. Concurrently, we observe that the peak associated with the stretching vibration mode of the C–O bonds in C–O–C α(1–6) links between anhydroglucose rings are significantly shifted toward higher wavenumbers (934 cm^{-1}) in the presence of [BMIM]Cl.

In the mean time, the maximum absorption peaks associated with the stretching vibration mode of the C–O bonds in C–O–H groups of starch do not show significant variations, taking into account the resolution of the spectrometer (1 cm^{-1}).

By analogy with the work of Hanke et al. (2002), we can assume the following schematic mechanism (the reality being probably more complex). Each ion pair Cl^-/$[BMIM]^+$ forms complex interactions with a C–O–H group of starch: the Cl^- anion strongly interacts with the hydrogen atom, while the $[BMIM]^+$ cation interacts with the oxygen atom. As a result, both the oxygen and the hydrogen atoms of the starch C–O–H group cannot form hydrogen bonds neither with water molecules nor with other O–H groups of starch. Therefore, intramolecular, intermolecular and hydration hydrogen bonds become softer. The overall result is a decrease of the hydrogen bonding intensity to which the hydrogen atoms of the O–H groups on average within the thermoplastic starch are submitted, explaining the shift towards higher wavenumbers of the O–H stretching vibration mode peak.

Such an interpretation suggests that [BMIM]Cl plasticized TPS would have less interactions with water molecules than glycerol plasticized TPS, which is supported by the decrease of water uptake described above.

The results obtained by Wang et al. (2009) suggest a different interaction mechanism in the case of [AMIM]Cl plasticized starch. Studying water solution cast starch films plasticized by [AMIM]Cl and/or glycerol (30 parts of plasticizer for 100 parts of starch), they observed that the Mid-infrared absorption peaks corresponding to the stretching vibration mode of C–O bonds of both C–O–H (around 1000 and 1150 cm^{-1}) and C–O–C groups (around 1020 and 1080 cm^{-1}) of starch are shifted to higher wavenumbers with increasing [AMIM]Cl. They concluded that the ionic liquid forms weaker hydrogen bonds than glycerol with the oxygen atoms of C–O–H and C–O–C groups of starch. From this conclusion, Wang et al. (2009) suggested that cations bearing hydroxyl groups should be used to enhance the plasticization of starch.

Table 4
Positions of the maxima of the main infrared absorption peaks of Fig. 3.

Sample	O–H stretch	C–O stretch (C–O–C groups of anhydroglucose rings)	C–O stretch (C–O–H groups)	C–O stretch (C–O–C links α(1–6))	
Native starch (granular)	3244	1077	–	1149	920–938
Starch film (casting)	3277	1075	1020	1150	924
[MC S100-G30]	3277	1078	1016	1150	926
[MC S100-G15-B15]	3293	1078	1017	1149	928
[MC S100-B30]	3306	1079	1021	1149	934
[EXT S100-G30]	3280	1076	1014	1149	925
[EXT S100-B30]	3323	1078	1019	1148	933

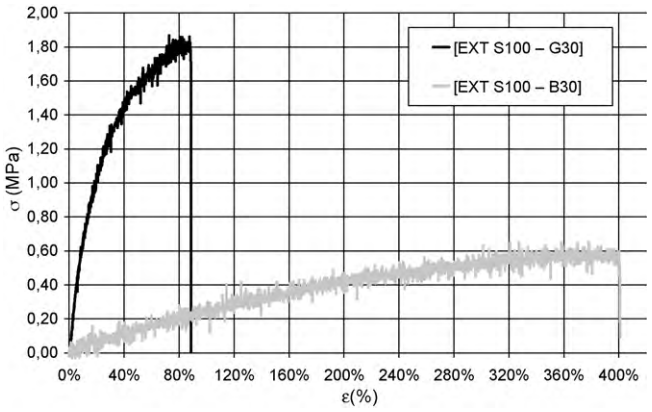

Fig. 4. Stress–strain curves obtained for the extruded samples.

At the same time, Wang et al. (2009) observed that the Mid-infrared absorption peaks corresponding to the stretching vibration mode of O–H bonds (around 3300 cm^{-1}) of intermolecular and intramolecular hydrogen bound hydroxyl groups of starch, water and glycerol are shifted towards lower wavenumbers with increasing [AMIM]Cl content. If we assume the probable strong interaction of Cl^- anions with the hydrogen atoms of the O–H groups, this suggests that on average, the O–H groups present in the material are more hydrogen bonded in the presence of [AMIM]Cl.

A possible interpretation of these observations, supported by the differences of electrical conductivity levels discussed above, is to assume that the ion pairs are dissociated in the case of [AMIM]Cl. In such a case, one Cl^- anion can interact locally with the hydrogen of one O–H groups of starch, while the $[AMIM]^+$ cation interacts weakly with the oxygen atom of another O–H group. In such a situation, the two O–H groups involved can still form hydrogen bonds with other O–H groups of starch or water. As a result, on average, the intensity of hydrogen bonding is increased. This interpretation is consistent with the observations of Wang et al. (2009) showing that [AMIM]Cl plasticized TPS samples are more hydrophilic than glycerol plasticized TPS (as opposed to what we observed in the case of [BMIM]Cl).

3.4. Functional properties of [BMIM]Cl plasticized starches

The electrical conductivity values of the two thermoplastic starches (Table 3) differ only by one order of magnitude. In the case of glycerol plasticized TPS, the "high" level of conductivity, compared to the results of Wang et al. (2009) is probably due to the presence of ionic impurities in the technical grade glycerol we used. More surprising is the "low" level of conductivity in the presence of [BMIM]Cl: $10^{-4.6}$ S/cm, while Wang et al. (2009) obtained a conductivity of $10^{-1.6}$ S/cm at 14.5 wt% water content in the presence of [AMIM]Cl for the same amount of ionic liquid. The ion pair dissociation mechanism of [AMIM]Cl described by Zhang et al. (2005), which does not take place in the case of [BMIM]Cl could increase the ion mobility and explain such high levels of conductivity in the case of [AMIM]Cl plasticized TPS, while ions remain more localized in the case of [BMIM]Cl plasticized TPS.

The results of the mechanical tensile tests presented in Fig. 4 and Table 3 confirm a strong plasticization of starch by [BMIM]Cl. The Young's modulus decreases by one order of magnitude compared to the classical glycerol plasticized TPS, while the elongation at break increases from 100% to 400%. According to the glass transition temperatures measured, both samples are in the rubbery state. Usually, for an amorphous polymer (without hydrogen bonds in the rubbery state), the rubbery Young's modulus should be 1 MPa. The much higher value for glycerol plasticized starch (8 MPa) could be explained by the presence of strong hydrogen bonds between the starch chains. In the presence of [BMIM]Cl, according to our interpretation of FTIR spectra, these intermolecular hydrogen bonds become weaker, leading to a more classical rubbery state modulus (0.5 MPa).

4. Conclusion

The ionic liquid 1-Butyl-3-methylimidazolium Chloride ([BMIM]Cl) was shown to be an efficient plasticizer of starch, allowing to produce thermoplastic starch (TPS) by melt processing. Two processing scales have been assessed: continuous twin screw extrusion and batch twin screw microcompounding, showing the feasibility of both. The later small processing scale opens the door for high-throughput studies of the interactions between starch (or other biopolymers) and ionic liquids as plasticizers and high-throughput studies of the properties of the resulting TPS materials, depending on the structure of the ionic liquids.

Actually, the structure of IL seems to play a key role, since some of the properties of the [BMIM]Cl plasticized TPS studied were radically different from those of starch films plasticized by a slightly different ionic liquid (1-allyl-3-methylimidazolium chloride [AMIM]Cl). The processing conditions probably also play an important role, since in the later case, the samples were obtained by casting from water solutions.

Electrically conducting [BMIM]Cl plasticized TPS obtained by twin screw extrusion is significantly less hydrophilic than glycerol plasticized TPS, taken as a reference. Both TPS samples present a molecular degradation occurred during the extrusion process, the order of magnitude of average molecular massed being in agreement with literature data about extrusion of starches with water or glycerol. The branching structures of plasticized TPS are similar and no short chains (DP < 12) are observed for both plasticizers. Nevertheless, the average molar mass is smaller in the case of [BMIM]Cl plasticized TPS, which could be related to a small derivatizing effect of the ionic liquid.

Despite the lower water uptake of [BMIM]Cl plasticized TPS, [BMIM]Cl acts as a much stronger glass transition temperature depressor than glycerol. Mechanical tensile tests confirm a strong plasticization of starch by [BMIM]Cl. The Young's modulus decreases by one order of magnitude compared to the glycerol plasticized TPS, while the elongation at break increases from 100% to 400%. The unusually low rubbery Young's modulus for [BMIM]Cl plasticized TPS (0.5 MPa) suggests a strong reduction of hydrogen bonds between the starch chains due to the presence of the ionic liquid. A detailed analysis by infrared spectroscopy supports this assumption, with the formation of strong hydrogen bonds between Cl^- anions and O–H group of starch, and the concurrent decrease of inter- and intra-molecular hydrogen bonds of starch chains.

Acknowledgments

The authors would like to thank Marion De Carvalho, Sophie Guilois, and Mickael Castro for their help in calorimetric, chromatographic and electrical conductivity measurements, respectively.

References

Anderson, J. L., Ding, J., Welton, T., & Armstrong, D. W. (2002). Characterizing ionic liquids on the basis of multiple solvation interactions. *Journal of the American Chemical Society*, *124*, 14247–14254.

Bello-Pérez, L. A., Roger, P., Baud, B., & Colonna, P. (1998). Macromolecular features of starches determined by aqueous high-performance size exclusion chromatography. *Journal of Cereal Science*, *27*, 267–278.

Biswas, A., Shogren, R. L., Stevenson, D. G., Willett, J. L., & Bhowmik, P. K. (2006). Ionic liquids as solvents for biopolymers: acylation of starch and zein protein. *Carbohydrate Polymers*, *66*, 546–550.

Bizot, H., LeBail, P., Leroux, B., Davy, J., Roger, P., & Buleon A. (1997). Calorimetric evaluation of the glass transition in hydrated, linear and branched polyanhydroglucose compounds. *Carbohydrate Polymers*, *32*(1), 33–50.

Brennecke, J. F., Rogers, R. D., & Seddon, K. R. (2007). Ionic liquids IV: Not just solvents anymore. In *ACS symposium series, Vol. 975* Washington DC: American Chemical Society.

Capron, I., Robert, P., Colonna, P., Brogly, M., & Planchot, V. (2007). Starch in rubbery and glassy states by FTIR spectroscopy. *Carbohydrate Polymers*, *68*(2), 249–259.

Couchman, P. R., & Karasz, F. E. (1978). A classical thermodynamic discussion of the effect of composition on glass-transition temperatures. *Macromolecules*, *11*, 117–119.

Finkenstadt, V. L., & Willett, J. L. (2004). Electroactive materials composed of starch. *Journal of Polymers and the Environment*, *12*(2), 43–46.

Flory, P. J. (1953). In P. J. Flory (Ed.), *Principles in polymer chemistry*. Ithaca, NY: Cornell University Press.

Fort, D. A., Remsing, R. C., Swatloski, R. P., Moyna, P., Moyna, G., & Rogers, R. D. (2007). Can ionic liquids dissolve wood? Processing and analysis of lignocellulosic materials with 1-n-butyl-3-methylimidazolium chloride. *Green Chemistry*, *9*, 63–69.

Fukaya, Y., Sugimoto, A., & Ohno, H. (2006). Superior solubility of polysaccharides in low viscosity, polar, and halogen-free 1,3-dialkylimidazolium formates. *Biomacromolecules*, *7*(12), 3295–3297.

Fukaya, Y., Hayashi, K., Wada, M., & Ohno, H. (2008). Cellulose dissolution with polar ionic liquids under mild conditions: Required factors for anions. *Green Chemistry*, *10*, 44–46.

Halley, P. J., Truss, R. W., Markotsis, M. G., Chaleat, C., Russo, M., Sargent, A. L., et al. (2008). A review of biodegradable thermoplastic starch polymers. In M. C. Celina, & R. A. Assink (Eds.), *Polymer durability and radiation effects. ACS symposium series*. Oxford (USA): Oxford University Press, pp 287–300.

Hanke, C. G., Atamas, N. A., & Lynden-Bell, R. M. (2002). Solvation of small molecules in imidazolium ionic liquids: a simulation study. *Green Chemistry*, *4*, 107–111.

Heinze, T., Dorn, S., Schöbitz, M., Liebert, T., Köhler, S., & Meister, F. (2008). Interactions of ionic liquids with polysaccharides. 2. Cellulose. *Macromolar Symposia*, *262*, 8–22.

Kilpeläinen, I., Xie, H., King, A., Grandstrom, M., Heikkinen, S., & Argyropoulos, D. (2007). Dissolution of wood in ionic liquids. *Journal of Agricultural Food Chemistry*, *55*, 9142–9148.

Lafargue, D., Pontoire, B., Buléon, A., Doublier, J. L., & Lourdin, D. (2007). Structure and mechanical properties of hydroxypropylated starch films. *Biomacromolecules*, *8*, 3950–3958.

Laus, G., Bentivoglio, G., Schottenberger, H., Kahlenberg, V., Kopacka, H., Röder, T., et al. (2005). Ionic liquids: current developments, potential and drawbacks for industrial applications. *Lenzinger Berichte*, *84*, 71–85.

Liu, Q, Janssen, M. H. A., van Rantwijk, F., & Sheldon, R. A. (2005). Room-temperature ionic liquids that dissolve carbohydrates in high concentrations. *Green Chemistry*, *7*, 39–42.

Lourdin, D., Coignard, L., Bizot, H., & Colonna, P. (1997). Influence of equilibrium relative humidity and plasticizer concentration on the water content and glass transition of starch materials. *Polymer*, *38*, 5401–5406.

Ma, X., Yu, J., & He, K. (2006). Thermoplastic starch plasticized by glycerol as solid polymer electrolytes. *Macromolecular Materials Engineering*, *291*, 1407–1413.

Moulthrop, J. S., Swatlowski, R. P., Moyna, G., & Rogers, R. D. (2005). High resolution ^{13}C NMR studies of cellulose and cellulose oligomers in ionic liquid solutions. *Chemical Communications*, *12*, 1557–1559.

Myllymäki, O., Eerikäinen, T., Suortii, T., Forssell, P., Linko, P., & Poutanen, K. (1997). Depolymerization of barley starch during extrusion in water glycerol mixtures. *Food Science and Technology – Lebensmittel-Wissenchaft & Technologie*, *30*(4), 351–358.

Myllymäki, V., & Aksela, R. (2005). Depolymerization method. *WO Pat.* No. 2005/066374A1.

Nishimura, N., & Ono, H. (2005). Preparation of novel polymer electrolytes using ionic liquid-modified starch. *Preprints of the Conference of the Chemical Soc of Japan (Nippon Kagakkai Koen Yokoshu)*, *85*(2), 1013.

Novoselov, N. P., Sashina, E. S., Petrenko, V. E., & Zaborsky, M. (2007). Study of dissolution of cellulose in ionic liquids by computer modelling. *Fibre Chemistry*, *39*(*2*), 153–158.

Piskin, E. (2002). Biodegradable polymers in medicine. In G. Scott (Ed.), *Degradable polymers: principles and applications* (p. 321). Dordrecht: Kluwer.

Planchot, V., Colonna, P., & Saulnier, L. (1997). In B. Godon, & W. Loisel (Eds.), *Guide Pratique d'Analyses dans les Industries des Céréales* (pp. 341–398). Paris, France: Lavoisier.

Remsing, R. C., Swatlowski, R. P., Rogers, R. D., & Moyna, G. (2006). Mechanism of cellulose dissolution in the ionic liquid 1-n-butyl-3-methylimidazolium chloride: a ^{13}C and $^{35/37}Cl$ NMR relaxation study on model systems. *Chemical Communications*, *12*, 1271–1273.

Robin, D., Rogers, R. D., Seddon, K. R., & Volkov, S. (2003). *Green industrial applications of ionic liquids*. Dordrecht, Boston: Kluwer Academic.

Roger, P., Bello-Pérez, L. A., & Colonna, P. (1999). Contribution of amylose and amylopectin to the light scattering behaviour of starches in aqueous solution. *Polymer*, *40*, 6897–6909.

Rogers, R. D., & Seddon, K. R. (2003). Ionic liquids-solvents of the future? *Science*, *302*, 792–793.

Rolland-Sabaté, A., Amani, N. G., Dufour, D., Guilois, S., & Colonna, P. (2003). Macromolecular characteristics of ten yam (Dioscorea spp.) starches. *Journal of the Science of Food and Agriculture*, *83*, 927–936.

Rolland-Sabaté, A., Colonna, P., Mendez-Montealvo, M. G., & Planchot, V. (2008). Online determination of structural properties and observation of deviations from power law behavior. *Biomacromolecules*, *9*, 1719–1730.

Sheldon, R. (2001). Catalytic reactions in ionic liquids. *Chemical Communications*, 2399–2407.

Stevenson, D. G., Biswas, A., Jane, J. L., & Inglett, G. E. (2007). Changes in structure and properties of starch of four botanical sources dispersed in the ionic liquid, 1-butyl-3-methylimidazolium chloride. *Carbohydrate Polymers*, *67*, 21–31.

Swatloski, R. P., Spear, S. K., Holbrey, J. D., & Rogers, R. D. (2002). Dissolution of cellulose with ionic liquids. *Journal of the American Chemical Society*, *124*, 4974–4975.

Swatloski, R. P., Rogers, R. D., & Holbrey, J. D. (2003). Dissolution and processing of cellulose using ionic liquids, *WO Pat.* No. 03/029329.

Van den Einde, R. M., van der Veen, M. E., Bosman, H., van der Goot, A. J., & Boom, R. M. (2004). Molecular breakdown of corn starch by thermal and mechanical effects. *Carbohydrate Polymers*, *56*, 415–422.

Van den Einde, R. M., Bolsius, A., van Soest, J. J. G., Janssen, L. P. B. M., van der Goot, A. J., & Boom, R. M. (2004). The effect of thermomechanical treatment on starch breakdown and the consequences for process design. *Carbohydrate Polymers*, *55*, 57–63.

Véchambre, C., Chaunier, L., & Lourdin, D. (2010). A novel shape-memory material based on potato starch. *Macromolecular Material and Engineering*, *295*, 115–122.

Wang, N., Zhang, X., Liu, H., & He, B. (2009). 1-Allyl-3-methylimidazolium chloride plasticized-corn starch as solid biopolymer electrolytes. *Carbohydrate Polymers*, *76*(*3*), 482–484.

Wang, N., Zhang, X., Liu, H., & Han, N. (2010). Ionically conducting polymers based on ionic liquid-plasticized starch containing lithium chloride. *Polymers & Polymer Composites*, *18*(1), 53–58.

Wyatt, P. J. (1992). In S. E. S. D. B. Harding, & V. A. Bloomfield (Eds.), *Laser light scattering in biochemistry* (pp. 35–58). Cambridge: The Royal Society of Chemistry.

Welton, T. (1999). Room-temperature ionic liquids. Solvents for synthesis and catalysis. *Chemical Reviews*, *99*(8), 2071–2084.

Xie, H., Zhang, S., & Li, S. (2006). Chitin and chitosan dissolved in ionic liquids as reversible sorbents of CO2. *Green Chemistry*, *8*, 630–633.

Yang, J. H., Yu, J. G., & Ma, X. F. (2006). Preparation of a novel thermoplastic starch (TPS). Material using ethylenebisformamide as the plasticizer. *Starch/Stärke*, *58*, 330–337.

Youngs, T. G. A., Holbrey, J. D., Deetlefs, M., Nieuwenhuyzen, M., Costa Gomes, M. F., & Hardacre, C. (2006). A molecular dynamics study of glucose solvation in the ionic liquid 1,3-dimethylimidazolium chloride. *ChemPhysChem*, *7*, 2279–2281.

Youngs, T. G. A., Hardacre, C., & Holbrey, J. D. (2007). Glucose solvation by the ionic liquid 1, 3-dimethylimidazolium chloride: A simulation study. *Journal of Physical Chemistry B*, *111*, 13765.

Zhang, H., Wu, J., Zhang, J., & He, J. S. (2005). 1-Allyl-3-methylimidazolium chloride room temperature ionic liquid: A new and powerful nonderivatizing solvent for cellulose. *Macromolecules*, *38*, 8272–8277.

Zhu, S., Wu, Y., Chen, Q., Yu, Z., Wang, C., Jin, S., et al. (2006). Dissolution of cellulose in ionic liquids and its application: A mini-review. *Green Chemistry*, *8*, 325–327.